

IET Generation, Transmission & Distribution

Special issue Call for Papers

**Be Seen. Be Cited.
Submit your work to a new
IET special issue**

Connect with researchers and experts in your field and share knowledge.

Be part of the latest research trends, faster.



Read more



The Institution of
Engineering and Technology

ORIGINAL RESEARCH

Operation strategies of battery energy storage systems for preventive and curative congestion management in transmission grids

Martin Lindner  | Jan Peper | Nils Offermann | Charlotte Biele | Milijana Teodosic |
Oliver Pohl  | Julian Menne | Ulf Häger

Institute of Energy Systems, Energy Efficiency and Energy Economics, TU Dortmund University, Dortmund, Germany

Correspondence

Martin Lindner, Institute of Energy Systems, Energy Efficiency and Energy Economics, TU Dortmund University, August-Schmidt-Str. 1, 44227 Dortmund, Germany.

Email: martin.lindner@tu-dortmund.de

Funding information

Large-Scale Equipment Initiative by the German Research Foundation (DFG), Grant/Award Number: 271512359; German Research Foundation (DFG): Open Access Costs

Abstract

Anticipating and relieving congestions is an ongoing challenge for transmission system operators. Distributed grid-scale battery energy storage systems enable operators to shift power flows and remedy congestion through virtual power lines and grid boosters. This paper includes battery energy storage systems in a combined preventive and curative congestion management optimization. First, it analyzes the impact of the two operational strategies in a case study of the German transmission grid. Furthermore, it outlines curative ad-hoc measures to overcome uncertainties during operational planning and real-time operation. The simulation results indicate that battery energy storage systems further increase the use of curative measures and reduce congestion management costs.

1 | INTRODUCTION

In times of large-scale integration of renewable energy sources (RES), transmission grids in many countries face new challenges since distances between load and generation are increasing, and weather conditions predominantly influence power flows. In some countries, such as Germany, this leads to enormous demand for additional transmission capacities. This demand is partly met by upgrading existing or installing new transmission lines. In addition, an increase in transmission capacities is possible by improving the existing transmission grid's utilization. Here, new assets such as Battery Energy Storage Systems (BESSs), owned and operated by the Transmission System Operators (TSOs), can make an impact. New operational concepts for BESSs can further improve the utilization of meshed transmission grids. For instance, by conducting curative Congestion Management (CM), it is possible to redirect power flows with fast activation of flexibilities right after an $(n-1)$ -contingency to eliminate potential overload in due time before transmission assets may overheat. Since BESSs can provide high flexibility, they are well suited for curative CM measures.

The main contribution of this paper is an analysis and comparison of the impact of BESSs on traditional preventive CM and a combination of preventive and curative CM, making it unique compared with the current state of the art in literature. Section 2 gives a detailed introduction to operational CM and the impact of BESSs, including delimitation from state-of-the-art implementations. Sections 4 and 5 present the models for BESSs and CM, respectively. Section 6 shows the simulation results of a study case based on the German electricity market setting and its transmission grid. Further added values by introducing a real-time CM system are derived in Section 7, followed by conclusions and a summary in Section 8.

2 | STATE OF THE ART IN CONGESTION MANAGEMENT USING BATTERY ENERGY STORAGE SYSTEMS

The capability of BESSs to switch between power consumption and generation, as well as the possibility to gradually and quickly

This is an open access article under the terms of the [Creative Commons Attribution-NonCommercial-NoDerivs](https://creativecommons.org/licenses/by-nc-nd/4.0/) License, which permits use and distribution in any medium, provided the original work is properly cited, the use is non-commercial and no modifications or adaptations are made.

© 2022 The Authors. *IET Generation, Transmission & Distribution* published by John Wiley & Sons Ltd on behalf of The Institution of Engineering and Technology.

change their set points, offers potential for their application in CM. This section illustrates recent applications.

2.1 | Congestion management

Market areas with centralized dispatch apply optimal power flow (OPF) calculations to optimize generation considering available transmission capacities. In contrast, the decentralized dispatch in Europe only depends on the market result in the respective bidding zones. Thus, TSOs may face frequent congestion in their grids. To operate the grid in an $(n-1)$ -secure way (considering single-outage contingencies), different types of CM measures are applied. The TSO's objective is to select and implement CM measures cost-efficiently and reliably [1]. Determining CM measures is part of daily operational planning processes that forecast upcoming grid situations. The implementation of CM measures is mainly directed from the control centre. Only a few decentralized power flow control schemes are implemented at the substation level.

Today's CM procedures plan and implement CM measures mainly preventively, that is, before the occurrence of a potential contingency that could cause line overloading. Preventive CM comprises grid-related, market-based, and emergency measures. Grid-related measures include adjusting operating points of power flow controlling assets, such as high-voltage direct current transmission systems (HVDC) or phase-shifting transformers (PSTs). Market-based measures include the redispatch of generation units and countertrading. Emergency measures can include load shedding or generation curtailment [2].

Upgrading transmission capacities is required to reduce costs for preventive CM measures. Apart from physical grid extensions, addressing operational transmission margins is necessary. A recent approach is to conduct CM measures curatively, that is, after the occurrence of a contingency [3, 4]. Acting curatively permits reducing transmission margins for incorporating power flow shifts in contingency situations. Hence, the usage of existing infrastructure under undisturbed conditions increases. Temporary exceedance of the Permanently Admissible Transmission Loading (PATL) is accepted as long as it does not put assets in danger of being damaged by high temperatures. Especially in the case of overhead line (OHL) conductors, their heat capacity leaves time to implement curative CM measures that reduce the loading before conductors reach their temperature limits. The power flow that results in reaching the maximal conductor temperature within a given curative timeframe is the so-called Temporary Admissible Transmission Loading (TATL). Operational guidelines allow TSOs to apply TATL limits during operational planning and real-time operation [2, 5].

Figure 1 visualizes how PATL and TATL constrain the power flow S_b on branch b during the undisturbed preventive CM phase and the curative timeframe after a contingency. The power flow S_b is assumed to change in a step-wise manner at the beginning and the end of the curative timeframe. This shape

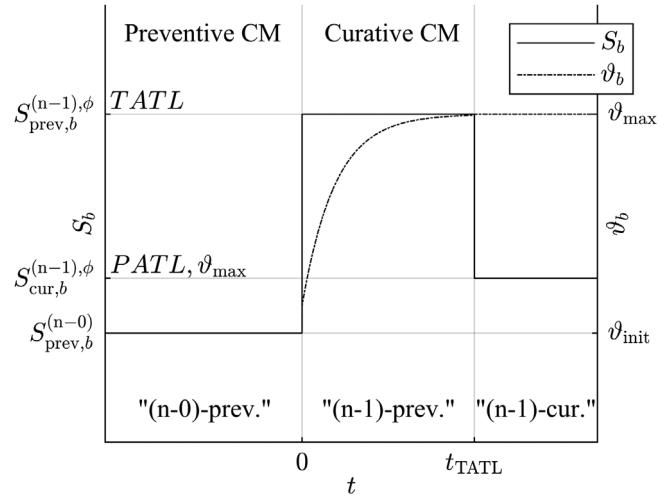


FIGURE 1 PATL and TATL constraints for the branch flow S_b during preventive ('prev') and curative ('cur') CM phases in $(n-0)$ - and $(n-1)$ -states. During the curative CM timeframe, the conductor temperature ϑ_b rises from ϑ_{init} to ϑ_{max} .

serves as a worst-case assumption for the thermal stress on the conductor.

To exploit transmission capacities effectively, PATL and TATL should consider weather conditions' influence on the transmission assets' ampacity (especially for OHL). Thermal conductor models, as proposed by IEEE [6] and CIGRE [7], are used for Dynamic Line Rating (DLR) based on the heat balance equation (HBE), which considers ambient conditions and the current on the conductor.

The relationship between the current and the resulting conductor temperature is non-linear, posing a challenge to CM optimization models formulated as linear (LPs) or mixed-integer linear problems (MILPs). Moreover, there exists no analytical solution to the HBE. Recent works demonstrated the integration of conductor temperature constraints into OPF problems [8–11]. The inclusion is either done by iteratively solving or simplifying the HBE. The authors of this paper used pre-calculated TATL and PATL and performed intermediate temperature evaluations during the CM optimization in [12]. The two consecutive curative timeframes have durations of 2 min and 13 min. The CM model presented in this paper effectively includes TATL constraints for one curative timeframe of 2 min without additional iterations to evaluate line temperatures. The method is presented in [13]. Moreover, the paper investigates the relevance of TATL limits for short curative timeframes.

2.2 | Battery energy storage systems for congestion management

While this paper focuses on grid operator-owned BESSs, various use cases exist for market participants and grid operators to use the flexibility provided by BESSs. An ongoing research topic is the location and sizing of storage. The authors of [14]

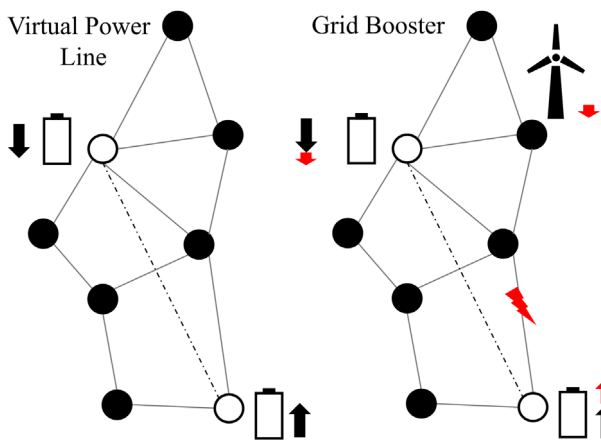


FIGURE 2 Visualization of virtual power line and grid booster. Arrows pointing upwards symbolize discharging of BESS. Arrows pointing downwards indicate the charging of BESS or curtailment of wind power generation. Preventive use is marked in black. Curative use after a contingency is marked in red.

co-optimized redispatch costs, as well as CAPEX and OPEX for grid operator-owned BESSs. The results for the German transmission grid in 2030 indicate that an exclusive use for preventive congestion management is not a viable business case. In [15], the authors compare different solutions for the long-term minimization of congestion in transmission grids due to wind power. The authors investigated combinations of DLR, BESSs, distributed static series compensators (DSSC), and grid reinforcement measures. The most economical solution was the combination of DLR and DSSC. This solution confirms that BESSs should not be solely applied for CM. Therefore, the suggested approach in [14] is the value-stacking of different use cases for BESSs, for example, avoidance of wind power curtailment as in [16–20]. Moreover, BESSs can provide ancillary services.

The following sections focus on the use of BESSs for CM purposes. First, the authors present two concepts for preventive use (virtual power line) and curative measures (grid booster). Figure 2 visualizes the two concepts.

2.2.1 | Virtual power line

This paper's authors refer to the virtual power line (VPL) as a concept of coordinated operation of two BESSs. The central objective is to relieve the AC grid while ensuring that the BESSs do not change the active power balance at any time to avoid market interference. The VPL allows shifting power flows over time, from time intervals with congestion to other time intervals in which sufficient transmission capacity is available on the lines. The VPL is part of preventive CM and does not interfere with energy markets. Although there is currently no explicit regulatory framework on VPL, various pilot projects test VPLs in electrical power grids. For example, the French TSO RTE pushes the VPL concept with a pilot of three BESSs [21]. A summary of ongoing VPL projects is listed in [22].

2.2.2 | Grid booster

BESSs are referred to as 'grid boosters' (GBs) when used in curative CM, that is, after a contingency. The authors of [23] introduced this concept. The mathematical base for including GBs in operational planning and real-time processes was developed in [24–27]. Finally, in [28], the authors outlined the integration steps for real-time operation particularly required for GBs. In contrast to the VPL, the counterpart for ensuring a balanced operation can also be flexible market-based units. The authors expect the market interference to be negligible because of the infrequent occurrence of contingencies. One counterpart option is using offshore wind (OW) farms connected via DC links to the AC grid since they are easily controllable by the system operator via the DC–AC inverters. The impact of GBs on voltage stability was investigated in [29]. The results indicate that GBs can be effectively applied even in grids with a high share of converter-based generation. It requires, however, sufficient reactive power capabilities. German TSOs will install three GB pilots connected at transmission and distribution grid levels by 2025 involving BESSs with a total rated power of 700 MW and a storage capacity of 700 MWh [30]. The regulator explicitly permitted these installations in the German Grid Development Plan [30].

3 | OUTLINE OF THE METHODS

The following chapters elaborate on the individual steps required to evaluate the usage of BESSs as VPL, GB, or as a curative ad-hoc measure (Figure 3). The operating points of the VPL are determined before the CM optimization. This decoupling is justifiable, as the VPL operation minimizes the overall loading of all lines, whereas the CM optimization minimizes the costs of individual CM measures.

4 | MODEL OF VIRTUAL POWER LINE

This section presents the optimization model of VPLs. The objective (1) minimizes the total relative congestion work E^{con} in the considered power system by optimizing the charging powers $P_{s,t}^{\text{Charge}}$ of the involved BESSs. The relative congestion work is the apparent power flow divided by the branch's maximum (DLR-adjusted) transmission capacity:

$$E^{\text{con}} = \min \left(\sum_{b \in \mathcal{M}_b} \sum_{t \in \mathcal{M}_t} e_{b,t}^{\text{con}} \right) \quad (1)$$

$$e_{b,t}^{\text{con}} = \max \left\{ \frac{|S_{b,t}^{\text{opt}}| - S_{b,t}^{\text{max}}}{S_{b,t}^{\text{max}}}, 0 \right\} \quad (2)$$

$$\forall t \in \mathcal{M}_t, \forall b \in \mathcal{M}_b$$

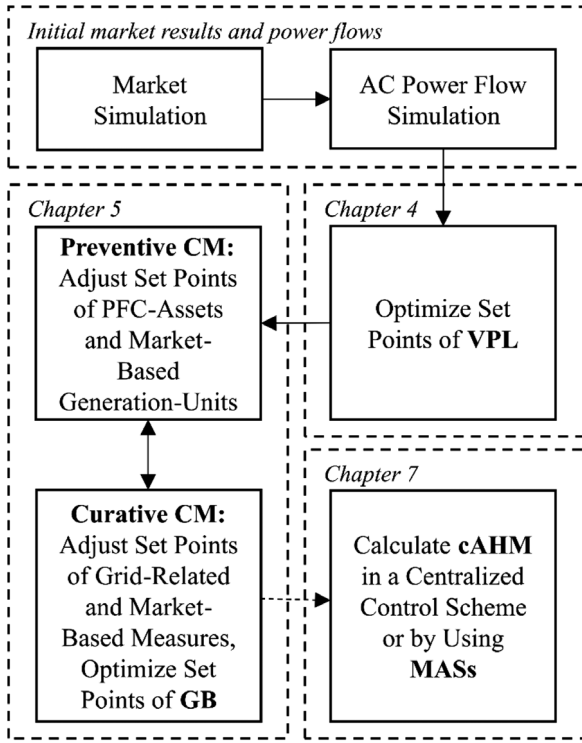


FIGURE 3 Process for evaluating the use of BESSs as VPL or GB

with

$$\mathcal{M}_b = \{1, \dots, b_{\max}\}, \quad \mathcal{M}_t = \{1, \dots, t_{\max}\} \quad (3)$$

whereby $e_{b,t}^{\text{con}}$ represents the relative congestion work on branch b at time t (2). The set of all considered branches is given by \mathcal{M}_b , the set of time points by \mathcal{M}_t (3).

The coupling between storage usage and power flow reduction of the AC branches is represented by (4). The power flow $S_{b,t}^{\text{opt}}$ on branch b at time t after optimization is the sum of the power flow before optimization $S_{b,t}^{\text{init}}$ and the power flow shifts created by the considered BESSs. The shifts are expressed as the product of the charging powers $P_{s,t}^{\text{Charge}}$ and the respective node-branch sensitivities $PIDF_{s,t}^{n \rightarrow b}$ (*Power Transfer Distribution Factors*) [31]. The index n represents the connection node of the BESS $s \in \mathcal{M}_s = \{1, \dots, s_{\max}\}$. The initial power flow $S_{b,t}^{\text{init}}$ is determined by an AC power flow calculation, considering the optimized operation of power flow-controlling devices, such as HVDC or PSTs.

$$S_{b,t}^{\text{opt}} = S_{b,t}^{\text{init}} + \sum_{s \in \mathcal{M}_s} PIDF_{s,t}^{n \rightarrow b} \cdot P_{s,t}^{\text{Charge}}, \quad (4)$$

$$\forall b \in \mathcal{M}_b, \forall t \in \mathcal{M}_t$$

with

$$PIDF^{n \rightarrow b} = \frac{\Delta S_b}{\Delta P_n}, \quad \forall b \in \mathcal{M}_b, \forall n \in \mathcal{M}_n \quad (5)$$

TABLE 1 Constraint description for VPL optimization

Equation	Description
(6)	The dispatch of all BESSs must equal out to avoid market interference.
(7)	The charging and discharging powers must be within the technical limits.
(8)	The state of charge (SoC) must not fall below the minimum or above the maximum allowed level.
(9)	The SoC is calculated for each timestep by adding the SoC of the previous timestep to the product of the mean charging power of the current timestep and the timestep length τ .
(10)	The initial SoCs of all storages are determined via the coefficient α_s based on the corresponding maximum capacity.

The optimization is limited by several constraints resulting from the technical boundaries of individual BESSs. These are described in (6) to (10) and explained in Table 1.

$$\sum_{s \in \mathcal{M}_s} P_{s,t}^{\text{Charge}} = 0, \forall t \in \mathcal{M}_t \quad (6)$$

$$P_s^{\min} \leq P_{s,t}^{\text{Charge}} \leq P_s^{\max} \quad (7)$$

$$\forall t \in \mathcal{M}_t, \forall s \in \mathcal{M}_s$$

$$0 \leq SOC_{s,t} \leq SOC_s^{\max} \quad (8)$$

$$\forall t \in \mathcal{M}_t, \forall s \in \mathcal{M}_s$$

$$SOC_{s,t} = SOC_{s,t-1} + P_{s,t}^{\text{Charge}} \cdot \tau, \quad (9)$$

$$\forall t \in \mathcal{M}_t, \forall s \in \mathcal{M}_s$$

$$SOC_{s,1} = \alpha_s \cdot SOC_s^{\max} \quad (10)$$

$$\forall s \in \mathcal{M}_s, \alpha_s \in [0, 1]$$

5 | CONGESTION MANAGEMENT MODEL

This section contains the mathematical formulation of the CM optimization problem. The CM optimization's objective is followed by the selection of cost factors and concludes with constraints for GBs and power flows.

5.1 | Objective

Congestion management measures are determined by minimizing the set point adjustments of power flow controlling assets and the redispatch of market-based generation units following the notations of [32, 33]. The objective in (11) considers both

preventive ('prev.') and curative terms ('cur.').

$$\min f(\mathbf{x}_{\text{prev}}, \mathbf{X}_{\text{cur}}) = \mathbf{c}_{\text{prev}}^T \cdot \mathbf{x}_{\text{prev}} + \mathbf{c}_{\text{cur}}^T \cdot \mathbf{X}_{\text{cur}} \quad (11)$$

s.t.

$$\mathbf{g}(\mathbf{x}_{\text{prev}}, \mathbf{X}_{\text{cur}}) \leq 0 \quad (12)$$

$$\mathbf{h}(\mathbf{x}_{\text{prev}}, \mathbf{X}_{\text{cur}}) = 0 \quad (13)$$

The constraints \mathbf{g} and \mathbf{h} will be detailed in Section 5.3. The vector \mathbf{x}_{prev} consists of the absolute preventive decision variables $\Delta \mathbf{p}_{\text{prev}}$ for redispatch measures of generation, load, and HVDC units, and $\Delta \boldsymbol{\theta}_{\text{prev}}$ for tap changes of PSTs.

$$\mathbf{x}_{\text{prev}} = \left[\begin{array}{c} \|\Delta \mathbf{p}_{\text{prev}}\| \\ \|\Delta \boldsymbol{\theta}_{\text{prev}}\| \end{array} \right] \quad (14)$$

$$\Delta \mathbf{p}_{\text{prev}} = [\Delta P_{\text{prev},1} \quad \cdots \quad \Delta P_{\text{prev},U}] \quad (15)$$

$$\Delta \boldsymbol{\theta}_{\text{prev}} = [\Delta \theta_{\text{prev},1} \quad \cdots \quad \Delta \theta_{\text{prev},P}] \quad (16)$$

The matrix \mathbf{X}_{cur} contains the absolute decision variables $\Delta \mathbf{P}_{\text{cur}}$ for curative redispatch measures of generation, load, and HVDC units $u \in \mathcal{M}_U = \{1, \dots, U\}$, and $\Delta \boldsymbol{\Theta}_{\text{cur}}$ for curative tap changes of PST $p \in \mathcal{M}_P = \{1, \dots, P\}$. Each row in \mathbf{X}_{cur} represents a unit/PST, and each column a possible contingency $\phi \in \mathcal{M}_\Phi = \{1, \dots, \Phi\}$ that is associated with a curative CM measure.

$$\mathbf{X}_{\text{cur}} = \left[\begin{array}{c} \|\Delta \mathbf{P}_{\text{cur}}\| \\ \|\Delta \boldsymbol{\Theta}_{\text{cur}}\| \end{array} \right] \quad (17)$$

$$\Delta \mathbf{P}_{\text{cur}} = \left[\begin{array}{ccc} \Delta P_{\text{cur},1}^1 & \cdots & \Delta P_{\text{cur},1}^\Phi \\ \vdots & \ddots & \vdots \\ \Delta P_{\text{cur},U}^1 & \cdots & \Delta P_{\text{cur},U}^\Phi \end{array} \right] = [\Delta \mathbf{p}_{\text{cur}}^1 \quad \cdots \quad \Delta \mathbf{p}_{\text{cur}}^\Phi] \quad (18)$$

$$\Delta \boldsymbol{\Theta}_{\text{cur}} = \left[\begin{array}{ccc} \Delta \theta_{\text{cur},1}^1 & \cdots & \Delta \theta_{\text{cur},1}^\Phi \\ \vdots & \ddots & \vdots \\ \Delta \theta_{\text{cur},P}^1 & \cdots & \Delta \theta_{\text{cur},P}^\Phi \end{array} \right] = [\Delta \boldsymbol{\theta}_{\text{cur}}^1 \quad \cdots \quad \Delta \boldsymbol{\theta}_{\text{cur}}^\Phi] \quad (19)$$

5.2 | Cost factors

Grid-related and market-based measures are used differently in preventive and curative CM. Due to the fast response times required, this paper only considers HVDC, PST, GB, and offshore-wind generation (OW) for curative CM measures. On the other hand, preventive CM measures comprise HVDC, PST, OW, RES, conventional generation ('Conv.'), must-run units,

and pumped storage power stations ('Hydro'). In addition, to ensure the solvability of the optimization problem, artificial load ('Load Management') and dummy units ('Dummy') are added to each node.

Graduated cost factors impose a prioritization of CM measures $\mathbf{c}_{\text{prev}}^T$ and $\mathbf{c}_{\text{cur}}^T$. The graduation ensures the regulatory precedence of non-costly, grid-related measures (HVDC, PST) over costly, market-based measures. RES and must-run units take priority over the redispatch of conventional units and pumped storage power stations. Binary start-up and shutdown decisions for generation units are implicitly modelled by imposing the high cost terms of must-run units in the power range of $[0; P_{\text{min}}]$. Consequently, the optimization problem retains an LP formulation. The set of potential units/PSTs considered for relieving congested branches is determined by minimum sensitivities. For nodal CM measures, PTDFs are used. Tap changes of PST are considered by Phase-Shift Distribution Factors (PSDF) [34], which denote the power flow change with respect to the phase shift due to tap changing under DC assumptions (no losses, flat voltage profile, only active power flows) [49]. This paper assumes minimum sensitivities $p_{tdf}^{\text{min}} = 0.05$ and $p_{sdf}^{\text{min}} = 1 \text{ MW}/1^\circ$.

As contingencies seldom occur, costs for curative measures are way smaller than costs for preventive measures. However, coordination efforts may decrease if a single preventive measure can replace multiple curative measures. The factor κ_{cont} separates the cost factors for preventive and curative measures from each other. Decision makers must choose this factor according to the grid's topology and the preference for curative versus preventive measures.

This paper assumes $\kappa_{\text{cont}} = 50$, that is, the optimizer would pick a preventive measure instead of applying a curative measure with the same sensitivity for at least 50 contingencies. Other grids may use smaller values depending on their size. Setting κ_{cont} to the maximum amount of possible contingencies enforces global precedence of curative measures over preventive measures at all times. However, this may lead to a wide spread of objective coefficients and numerical issues during the solving process.

The units' specific marginal costs $\mathbf{c}_{\text{conv}} \in \mathbb{R} : [c_{\text{conv}}^{\text{min}}, c_{\text{conv}}^{\text{max}}]$ graduate redispatch costs of conventional power plants. In this paper $c_{\text{conv}}^{\text{min}} = 37 \frac{\text{€}}{\text{MW}}$ and $c_{\text{conv}}^{\text{max}} = 160 \frac{\text{€}}{\text{MW}}$. This range is the starting point for calculating the other cost factors shown in Table 2.

5.3 | Constraints

The equality constraints $\mathbf{h}(\mathbf{x}_{\text{prev}}, \mathbf{X}_{\text{cur}})$ and inequality constraints $\mathbf{g}(\mathbf{x}_{\text{prev}}, \mathbf{X}_{\text{cur}})$ consist of unit- and grid-related constraints. The possible redispatch range of generation units is limited by the asset-specific operation boundaries and the maximum slopes, as shown in (20) and (21), respectively.

$$P_u^{\text{min}} \leq P_{\text{init},u} + \Delta P_{\text{prev},u} \leq P_u^{\text{max}} \quad (20)$$

TABLE 2 Prioritization of CM measures and associated cost factors in the optimization problem

Prio.	CM measure	Cost factor	Value
1	prev. HVDC, prev. PST, cur. HVDC, cur. PST, cur. GB	$c_{\text{conv}}^{\min} \cdot \frac{ptd_j^{\text{min}^2}}{k_{\text{cont}}}$	$1.9 \cdot 10^{-3}$
2	cur. OW	$c_{\text{conv}}^{\min} \cdot \frac{ptd_j^{\text{min}}}{k_{\text{cont}}}$	$3.7 \cdot 10^{-2}$
3	prev. Conv, prev. Hydro	c_{conv}	[37, 160] unit-specific
4	prev. RES, OW, Must-Run	$c_{\text{conv}}^{\max} \cdot \frac{1}{ptd_j^{\text{min}}}$	$3.2 \cdot 10^3$
5	prev. Dummy	$c_{\text{conv}}^{\max} \cdot \frac{1}{ptd_j^{\text{min}^2}}$	$6.4 \cdot 10^4$
6	prev. Load Management	$c_{\text{conv}}^{\max} \cdot \frac{1}{ptd_j^{\text{min}^3}}$	$1, 3 \cdot 10^6$

$$\Delta P_u^{\min} \leq \Delta P_{\text{prev},u} \leq \Delta P_u^{\max} \quad (21)$$

$$\forall u \in \mathcal{M}_U$$

The phase shift angles of PSTs are constrained by (22).

$$\theta_p^{\min} \leq \theta_{\text{init},p} + \Delta \theta_{\text{prev},p} \leq \theta_p^{\max} \quad (22)$$

$$\forall p \in \mathcal{M}_P$$

Additionally, (23), (24), and (25) define the curative asset-specific constraints.

$$P_u^{\min} \leq P_{\text{init},u} + \Delta P_{\text{prev},u} + \Delta P_{\text{cur},u}^{\phi} \leq P_u^{\max} \quad (23)$$

$$\Delta P_u^{\min} \leq \Delta P_{\text{cur},u}^{\phi} \leq \Delta P_u^{\max} \quad (24)$$

$$\forall u \in \mathcal{M}_U, \forall \phi \in \mathcal{M}_{\Phi}$$

$$\theta_p^{\min} \leq \theta_{\text{init},p} + \Delta \theta_{\text{prev},p} + \Delta \theta_{\text{cur},p}^{\phi} \leq \theta_p^{\max} \quad (25)$$

$$\forall p \in \mathcal{M}_P, \forall \phi \in \mathcal{M}_{\Phi}$$

In addition, inverters of HVDC links must have inverse operating points at all times. Furthermore, Section 5.3.2. describes additional modelling assumptions for GB units in detail.

Positive and negative redispatch measures must cancel each other out to ensure a balanced operation ((26) and (27)).

$$\sum_{u=1}^U \Delta P_{\text{prev},u} = 0 \quad (26)$$

$$\sum_{u=1}^U \Delta P_{\text{cur},u}^{\phi} = 0 \quad \forall \phi \in \mathcal{M}_{\Phi} \quad (27)$$

This paper imposes power flow constraints on OHLs and cables only as they are the most restricting assets in the transmission grid. Transformers and substation equipment are neglected as they are assumed to be exchangeable according to the transmission needs.

TABLE 3 CM states and corresponding power flow limits

State	Period	Description	Limit
'init'	Before operational planning	Market results without CM measures	-
'(n-0)-prev.'	$t \leq 0$	No contingency, after prev. CM	PATL
'(n-1)-prev.'	$0 \leq t \leq t_{\text{TATL}}$	Contingency, after prev. CM	TATL
'(n-1)-cur.'	$t \geq t_{\text{TATL}}$	Contingency, after prev. and cur. CM	PATL

Depending on the contingency status of the grid and the point in time t , different power flow limits apply (Table 3). Refer to Figure 1 for visualization. Right after the occurrence of a contingency at $t = 0$ curative measures are activated and come into effect by $t = t_{\text{TATL}}$. During this period, TATL limits apply, which allow for temporarily increased power flow limits. Section 5.3.1 elaborates on how to determine PATL and TATL values.

The constraints for the '(n-0)-prev.'-state are stated as follows:

$$s_{\text{prev}}^{(n-0)} = s_{\text{init}} + PTDF \cdot \Delta p_{\text{prev}} + PSDF \cdot \Delta \theta_{\text{prev}} \quad (28)$$

$$-s_b^{\text{PATL}} \leq s_{\text{prev},b}^{(n-0)} \leq s_b^{\text{PATL}} \quad (29)$$

$$\forall b \in \mathcal{M}_B$$

The shift of power flows due to a contingency is quantified by linear Line Outage Distribution Factors (LODFs) [35]. The variable $s_{\text{prev},b}^{(n-1),\phi}$ represents the power flow on branch b after implementing preventive CM measures and an outage of branch ϕ . Equations (30) and (31) describe the '(n-1)-prev.'-constraints:

$$s_{\text{prev},b}^{(n-1),\phi} = s_{\text{prev},b}^{(n-0)} + lodf_{b,\phi} \cdot s_{\text{prev},\phi}^{(n-0)} \quad (30)$$

$$-s_b^{\text{TATL}} \leq s_{\text{prev},b}^{(n-1),\phi} \leq s_b^{\text{TATL}} \quad (31)$$

$$\forall b \in \mathcal{M}_B, \forall \phi \in \mathcal{M}_{\Phi}$$

After the contingency of branch ϕ , the PTDF sensitivities of nodes and the PSDF sensitivities of PST on branches change in the following way:

$$OTDF^{\phi} = PTDF + lodf^{\phi} \cdot ptdf^{\phi} \quad (32)$$

$$OSDF^{\phi} = PSDF + lodf^{\phi} \cdot psdf^{\phi} \quad (33)$$

$$\forall \phi \in \mathcal{M}_{\Phi}$$

The sensitivity matrices $OTDF^{\phi}$ (Outage Transfer Distribution Factor) and $OSDF^{\phi}$ (Outage Phase Shift Distribution Factor) are constructed from the initial $PTDF$ and $PSDF$

matrices, and the column vector $\mathit{lod} f^\phi$, which is the ϕ th column of LODF , and the row vectors $\mathit{ptd} f^\phi$ and $\mathit{psd} f^\phi$, which are the ϕ th row of PTDF and PSDF , respectively.

The branch flows during the ‘(n-1)-cur.’-state equate to (34) and (35).

$$\mathit{s}_{cur}^{(n-1),\phi} = \mathit{s}_{prev}^{(n-1),\phi} + \mathit{OTDF}^\phi \cdot \Delta \mathit{p}_{cur}^\phi + \mathit{OSDF}^\phi \cdot \Delta \theta_{cur}^\phi \quad (34)$$

$$\begin{aligned} -\mathit{s}_b^{\mathit{PATL}} &\leq \mathit{s}_{cur,b}^{(n-1),\phi} \leq \mathit{s}_b^{\mathit{PATL}} \\ \forall b \in \mathcal{M}_B, \forall \phi \in \mathcal{M}_\Phi \end{aligned} \quad (35)$$

5.3.1 | PATL and TATL constraints

The permanently and temporarily admissible transmission loading represents the minimum of several factors that may limit the transmission capability:

1. System stability limits
2. Protection limits
3. Thermal limits
4. Electromagnetic interference
5. External limits

The listed limitations result in a permissible current I_b^{PATL} but can be transformed into power flow limits $\mathit{s}_b^{\mathit{PATL}}$ after obtaining the voltages $U_{b,1}$ and $U_{b,2}$ at a branch’s start and end node by conducting an AC power flow calculation (36).

$$\begin{aligned} \mathit{s}_b^{\mathit{PATL}} &= \sqrt{3} \cdot I_b^{\mathit{PATL}} \cdot \min(U_{b,1}, U_{b,2}) \\ \forall b \in \mathcal{M}_B \end{aligned} \quad (36)$$

The application of DLR, which adjusts thermal limits according to real-time or forecasted weather conditions, is currently implemented by all German TSOs. DLR permits to increase in the nominal ampacity of OHL conductors by up to 50% relative to worst-case standard conditions [36]. An overall limit of 3.6 kA is currently active due to concerns about protection devices and electromagnetic interference with pipeline infrastructure. Although this limit may increase in the near future, this paper considers PATL currents I_b^{PATL} according to the outlined policies.

Depending on the simulation scenario in Section 6, TATL values may be either unlimited or restricted by thermal or external limits. Neglecting external limitations may be justifiable, as the authors assume $t_{\mathit{TATL}} = 2$ min, which is a reasonably short reaction time to activate curative CM measures by means of automation. Moreover, contingencies involving significant usage of TATL potentials are assumed to be very seldom.

The thermal reserve of overhead lines highly depends on their initial conductor temperature. The higher the power flow $\mathit{s}_{prev,b}^{(n-0)}$ during the ‘(n-0)-prev.’-state, the lower the thermal reserve for curative CM. The TATL value $\mathit{s}_b^{\mathit{TATL}}$ therefore is

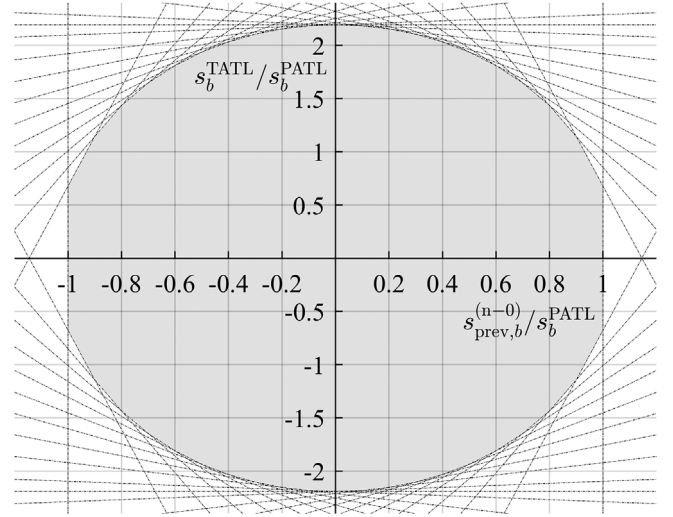


FIGURE 4 Feasible set of TATL-PATL-ratio depending on the base loading after preventive CM approximated by linear constraints for 264-AL1/34-ST1A conductor with $t_{\mathit{TATL}} = 2$ min, $\vartheta_{\max} = 80^\circ\text{C}$, 0.6 m/s wind speed (perpendicular), 35°C ambient temperature and 900 W/m^2 solar irradiation, 5 K fault current heating [13]

a function of $\mathit{s}_{prev,b}^{(n-0)}$.

$$\begin{aligned} \mathit{s}_b^{\mathit{TATL}} &= f\left(\mathit{s}_{prev,b}^{(n-0)}\right) \\ \forall b \in \mathcal{M}_B \end{aligned} \quad (37)$$

Due to the non-linear nature of standard thermal conductor models proposed by IEEE [6] and CIGRE [7], the direct inclusion of thermal constraints in the CM model would turn the original linear into a non-linear optimization problem. To overcome this issue, $\mathit{s}_b^{\mathit{TATL}}$ is determined for different pre-loading values assuming fixed weather conditions for each branch, and $t_{\mathit{TATL}} = 2$ min.

$$\begin{aligned} \mathit{s}_{prev,b}^{(n-0)} &= \mathit{s}_b^{\mathit{PATL}} \cdot \mathit{k}_{prev}^{(n-0)} \\ \forall b \in \mathcal{M}_B, \mathit{k}_{prev}^{(n-0)} &\in \mathbb{R} : [0, 1] \end{aligned} \quad (38)$$

The tool used to calculate the TATL values according to [6] is described in [13]. An exemplary curve of the admissible TATL-PATL-ratio $\mathit{k}_{\mathit{TATL}} = \mathit{s}_b^{\mathit{TATL}} / \mathit{s}_b^{\mathit{PATL}}$ depending on the base loading $\mathit{k}_{\mathit{PATL}} = \mathit{s}_{prev,b}^{(n-0)} / \mathit{s}_b^{\mathit{PATL}}$ is depicted in the first quadrant of Figure 4 for $\mathit{k}_{\mathit{PATL}} = \{0, 0.1, \dots, 1\}$. This approach was proposed in [13]. Accordingly, this paper adds a 5 K temperature step to the initial pre-fault conductor temperature to incorporate the heating induced by short-circuit currents. Hence, $\mathit{k}_{\mathit{TATL}} < 1$ at $\mathit{k}_{\mathit{PATL}} = 1$, which prevents branches affected by power flow shifts due to contingencies from being operated close to 100% loading in (n-0)-state.

By mirroring the first quadrant’s curve at the abscissa and the ordinate, a convex set for all feasible combinations of $\mathit{k}_{\mathit{PATL}}$ and $\mathit{k}_{\mathit{TATL}}$ is returned. The non-linear boundary can be approximated by an array of linear functions of type $f(x) = \mathit{k}x + n$.

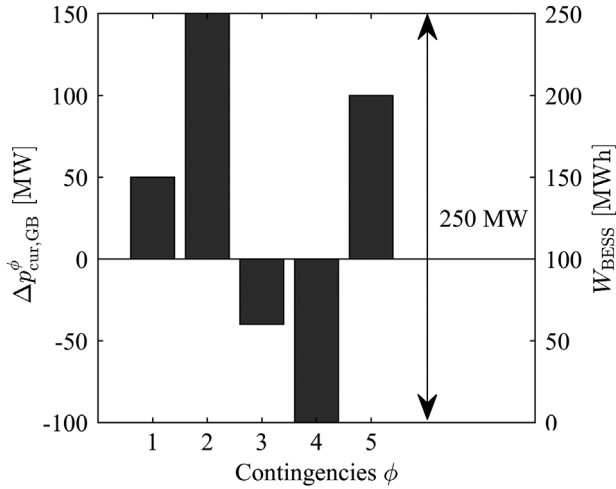


FIGURE 5 Limited range for curative grid booster operating points $\Delta p_{\text{cur,GB}}^{\phi}$ to facilitate the storage capacity limit of $W_{\text{max}} = 250$ MWh for an operation time of $t_{\text{GB}} = 1$ h. The depicted bars apply to both y-axes.

Each function contains two points that can be calculated and stored in a lookup table before the CM optimization for the corresponding conductor, weather conditions, and base load values (39).

$$s_b^{\text{TATL}} = f \left(s_{\text{prev},b}^{(n-0)} \right) = s_{\text{prev},b}^{(n-0)} \cdot k + n \quad (39)$$

$$\forall b \in \mathcal{M}_B$$

Thus, the constraint expressed in (31) is applied as often as approximate linear functions are constructed.

5.3.2 | Grid booster constraints

Although the optimization statement neglects temporal couplings between points in time, the storage capacity of BESSs must be considered in a simplified manner to avoid an overestimation of the feasible operational range. Pilot projects for GB in Germany assume that the BESS is capable of charging and discharging at rated power for $t_{\text{GB}} = 1$ h (e.g. $P_r = 250$ MW and $W_{\text{max}} = 250$ MWh) [30]. Depending on the contingencies that can happen at one point in time, the GB may be allocated for charging and discharging during operational planning. In any contingency, the storage boundaries must not be exceeded. Figure 5 provides an example.

Equation (40) describes the possible power range of all curative GB operating points.

$$P_{\text{range}} = \frac{W_{\text{max}}}{t_{\text{GB}}} \quad (40)$$

All GB units are assigned a range constraint described by (41).

$$\max \Delta p_{\text{cur},\mu}^{\phi} - \min \Delta p_{\text{cur},\mu}^{\phi} \leq P_{\text{range}} \quad (41)$$

$$\forall \phi \in \mathcal{M}_{\Phi}, \forall \mu \in \mathcal{M}_{\text{GB}} \subset \mathcal{M}_U$$

By splitting $\Delta p_{\text{cur},\mu}^{\phi}$ into a positive part $\Delta p_{\text{cur},\mu}^{\phi,+}$ and a negative part $\Delta p_{\text{cur},\mu}^{\phi,-}$ (41) can be transformed by the \mathcal{L}_{∞} -norm: $\|x\|_{\infty} = \max(|x_1|, \dots, |x_n|)$.

$$\left\| \Delta p_{\text{cur},\mu}^{\phi,+} \right\|_{\infty} + \left\| \Delta p_{\text{cur},\mu}^{\phi,-} \right\|_{\infty} \leq P_{\text{range}} \quad (42)$$

$$\forall \phi \in \mathcal{M}_{\Phi}, \forall \mu \in \mathcal{M}_{\text{GB}} \subset \mathcal{M}_U$$

5.4 | Iterative contingency selection

Including the constraints for all possible critical outages/contingencies (CO) and critical branches (CB) in the CM optimization leads to large memory requirements. According to [33], an iterative approach conducts a contingency analysis after each CM optimization run. It adds combinations of CBs and COs to the optimization problem according to the following criteria:

1. CBs overloaded in ‘(n-0)-prev.’-state
2. CB-CO-combinations that yield the highest overload in the ‘(n-1)-prev.’-state per CB
3. All overloaded CB-CO-combinations in ‘(n-1)-cur.’-state

The new set of unique CB-CO combinations applies to all preventive and curative states in the upcoming iteration. Once no more congestions occur, the final CM result is valid.

6 | SIMULATION RESULTS

This study case investigated the concepts for VPLs and GBs based on the German transmission grid for 2030. First, the grid model, including the VPL, is presented in Section 6.1. Subsequently, Section 6.2 summarizes the investigated scenarios. Finally, Section 6.3 compares the simulation results with particular regard to the role of TATL constraints and the effectiveness of curative measures.

6.1 | Grid model and virtual power line

The presented concepts were implemented in the market and network simulation environment Model of International Energy Systems (MILES), according to the B2030 scenario of the German Grid Development Plan created in 2019 [37]. The European countries were modelled with corresponding scenarios of the Ten-Year Network Development Plan (TYNDP) [38]. Using MILES, the individual loads and generation units were first regionalized at the European and German levels, and individual units’ behaviours over time were subsequently determined. Based on the weather year 2012, time series of weather-dependent generation and loads were generated. The dispatch of the European power plant fleet was determined by mixed-integer unit commitment optimization. The resulting nodal powers were assigned to the network model for power flow calculations. The European transmission network model

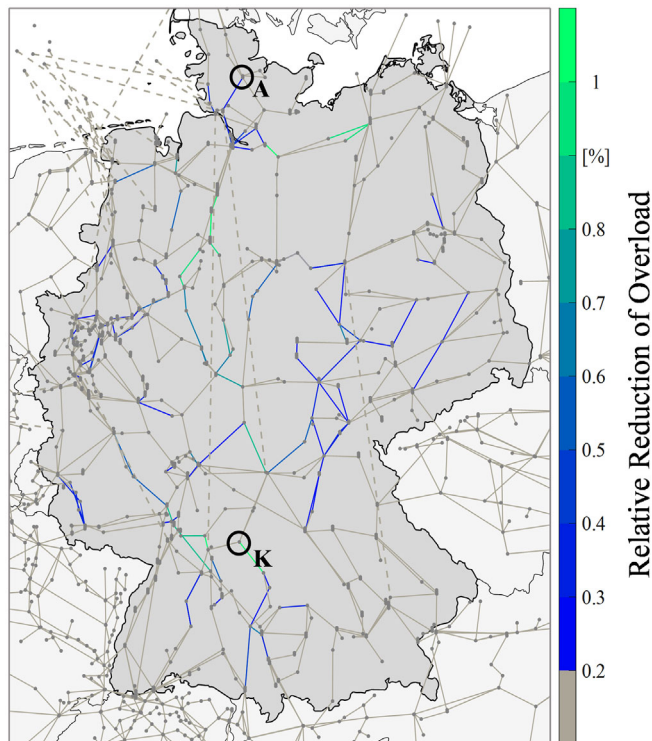


FIGURE 6 Relative reduction of $(n-0)$ -overload in German transmission grid after usage of BESSs in Audorf (A) and Kupferzell (K) as VPL

includes approximately 4000 nodes and 6000 branches. The network model contains system components greater than or equal to the 220-kV voltage level, for example, AC lines, transformers, and power flow controlling devices such as HVDC lines and PST. In addition to the grid expansion measures already being realized, the German Federal Requirements Plan measures were modelled. A detailed description of the grid model and the energy system model MILES was presented in [39].

The locations of the BESSs were chosen according to the German Grid Development Plan [30] as Audorf (A) and Kupferzell (K). Figure 6 visualizes the locations. Congested transmission corridors were mainly present in the northern and central parts of Germany due to high wind generation in the north and industrial loads in the south. BESS K was a 250 [MW, MWh] storage intended to be used with OW curtailment as a counterpart. BESS A is actually part of a pilot involving two 100 [MW, MWh] storages. Its counterpart was located southwest of BESS K.

It was assumed that both BESSs have a capacity of 250 MWh each and a rated power of 250 MW, simplifying the VPL operation optimization and permitting an hourly resolution for the CM optimization. Since these BESS rely on lithium-ion technology, it was assumed that they can both charge and discharge their total capacity within a single timestep of the VPL optimization. While the efficiency of the BESS was neglected in the optimization, a subsequent analysis of the determined operating points showed total losses of approx. 50 GWh/a (on average 5.69 MW) per storage if a round-trip efficiency of 90%

TABLE 4 Investigated simulation scenarios

Scenario	Prev. CM	Cur. CM	VPL	TATL
0a	No	No	No	No
0b	No	No	Yes	No
1	Yes	No	No	No
2	Yes	No	Yes	No
3a	Yes	Yes	Yes	External limits
3b	Yes	Yes	Yes	Only thermal limits
3c	Yes	Yes	Yes	Unlimited
4	Yes	Yes	No	Only thermal limits

was assumed. Therefore, neglecting the efficiency factors in the model seems reasonable.

In addition, both BESSs could curatively interact with each other and OW curtailment when used as GBs.

Figure 6 provides an overview of the area affected by the storage systems operated as VPLs. The storage units mainly affected the area between them, whereby the maximum loading of numerous lines was reduced by up to 1%.

6.2 | Investigation scenarios

The study case comprised different scenarios (Table 4) that addressed the influences of curative CM, VPLs, GBs, and TATL constraints on CM results.

In case the BESSs were used as VPL and GB, the VPL operating points were assumed fixed, leaving the remaining capacity for curative purposes of the GB. The CM optimization comprised 8760 grid utilization cases (GUCs), each representing 1 h of a year.

Scenarios 3a, 3b, and 3c focussed on the influence of TATL constraints. Scenario 3a caps TATL at 3.6 kA or $1.5 \cdot PATL$ to incorporate external limits. Scenario 3b determined TATL solely based on thermal limits. In Scenario 3c, no TATL limit was applied within $0 \leq t \leq t_{TATL}$. Scenario 4 does not contain the VPL, so the BESSs are used for curative CM only.

All GUCs were solved independently. Neglecting the time coupling between GUCs allowed for a parallelized application of the CM algorithm. However, the missing time coupling may have overestimated the flexibility of conventional power plants and pumped hydroelectric energy storage units. The CM optimization considered 750 COs and 644 CBs, 639 of which were assigned TATL constraints.

6.3 | Simulation results

The main criterion for evaluating the effect of grid expansion measures and operational flexibilities is the preventive redispatch volume (Figure 7).

Scenario 1 set the reference value of 12.84 TWh for purely preventive CM. Only a slight reduction to 12.81 TWh was made

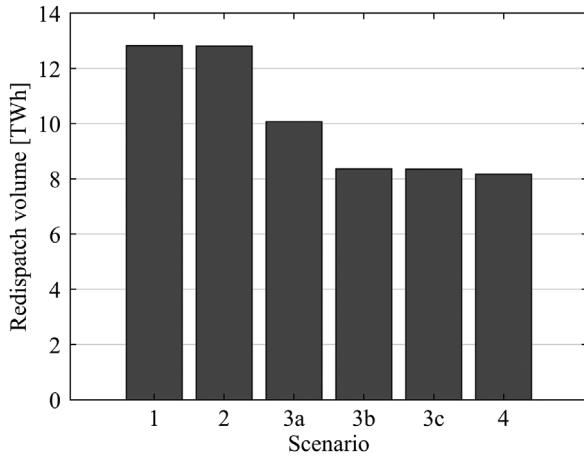


FIGURE 7 Comparison of preventive redispach volumes

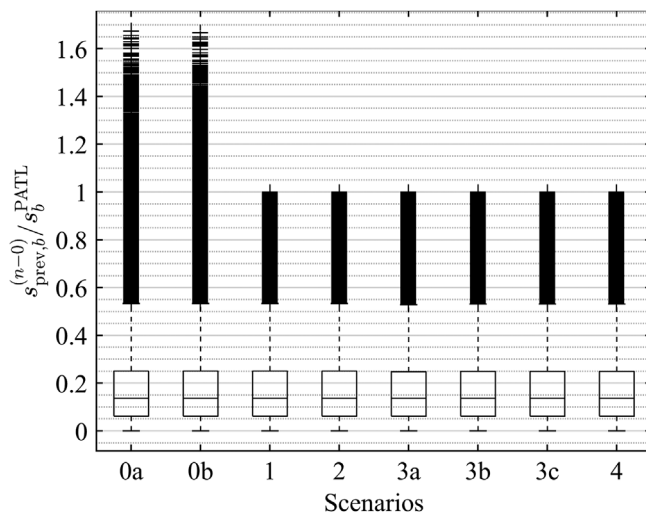


FIGURE 8 $(n-0)$ -loading (relative to PATL) of 644 CBs without CM (Scenarios 0a and 0b) and after preventive CM (Scenarios 1 to 4) for 8760 GUCs

possible by the VPL. Introducing curative measures in Scenario 3a allowed for a decrease to 10.06 TWh (-21.6%). Without capping TATL values in Scenario 3b, the redispach volume decreased to 8.37 TWh (-34.8%). Just a minor improvement was possible in Scenario 3c (8.35 TWh), indicating that TATL constraints in Scenario 3b were only rarely binding. Applying BESSs only for curative CM decreased the redispach volume to 8.17 TWh (-36.3%). With the provided BESS sizes and locations, it is hence preferable to use them merely for curative CM purposes instead of for a VPL.

Another comparison dimension is the loading of branches relative to their PATL. Figure 8 summarizes the $(n-0)$ -loading values of the critical branches for all 8760 GUCs in boxplots. Scenarios 0a and 0b are displayed for comparison. The most severe $(n-0)$ -overload reached up to 167%. Depending on the scenario, CM measures were applied in 6359 to 6385 of 8760 GUCs. Still, the overall loading distribution only changed

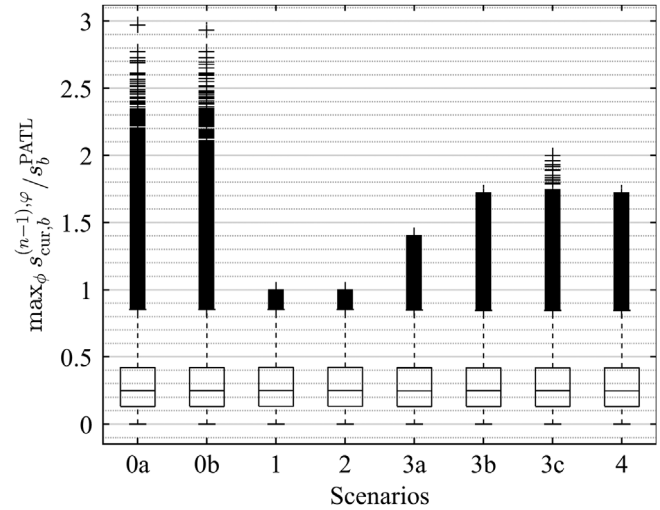


FIGURE 9 Maximal $(n-1)$ -loading (relative to PATL) per branch and GUC after preventive CM (except for scenarios 0a and 0b). Depending on the scenario, 6359 to 6385 GUCs with CM, 750 COs, and 644 CBs were considered.

TABLE 5 TATL usage statistics

Scenario	3a	3b	3c	4
Percentage of considered GUCs with TATL usage	88.2%	95.1%	95.1%	96.0%
Percentage of considered contingencies limited by TATL	15.6%	2.5%	-	2.6%
Branches with used TATL at least once	148	206	-	206
Branches limited by TATL at least once	106	43	-	41

at its borders. In addition, no significant rise in the median $(n-0)$ -loading was observed.

Figure 9 depicts boxplots of the maximal $(n-1)$ -loading per branch and GUC. Again, except for the outliers, the medians, quartiles, and whiskers remained almost equal for all scenarios.

Scenarios 0a and 0b had several branches which would have been heavily overloaded in the $(n-1)$ -state without CM measures. The comparison of the maximum $(n-1)$ -loading in scenarios 3a (140%), 3b (172%), and 3c (200%) reveals the effect of different TATL limitations. Neglecting the thermal TATL limitation in 3c led to inadequate power flows for only 18 of $4.1 \cdot 10^6$ CBs considered in the GUC-specific CM optimizations.

To underline the importance of the degree of freedom offered by a 2-min timeframe for curative CM, Table 5 summarizes the usage of TATL capabilities for scenarios 3a, 3b, 3c, and 4. For more than 88.2% of all GUCs which require CM, at least one contingency occurs that leads to an exceedance of PATL. The percentage of all considered contingencies which lead to binding TATL constraints for at least one branch decreases from 15.6% in Scenario 3a to 2.6% in Scenario 4. Although 639 branches were assigned TATL constraints, this capability was

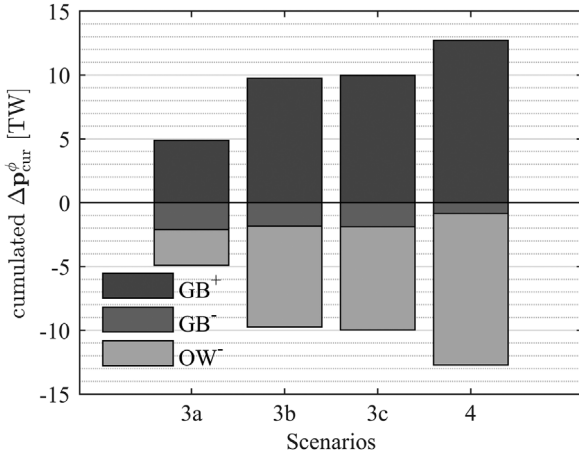


FIGURE 10 Cumulated curative adjustments of GB and OW units

only exploited by up to 206 branches, of which only 41 (Scenario 4) to 106 (Scenario 1) became constraining for the CM optimization problem.

Following the results of Figures 7–9, and Table 5, neglecting TATL values determined solely based on thermal considerations for a 2-min curative timeframe appears justifiable. However, additional limiting factors or longer curative timeframes may require properly including thermal TATL constraints in the CM optimization.

The impact of external limiting factors is also observable in the cumulated curative adjustments of GB and OW infeed (Figure 10). The total amount doubles from 10 TW (Scenario 3a) to 20 TW (Scenario 3c). When BESSs were only used for GB purposes in Scenario 4, the cumulated adjustments peaked at 25.4 TW.

Another observation from Figure 10 is that GBs predominantly feed in power. The most prominent counterpart was OW. Thus, contingencies existed for which both GBs fed in power while OW was curtailed. Hence, ramping up GBs was beneficial to maximize the relieving effect of OW curtailment.

An inspection of the VPL and GB set points in Figure 11 reveals that the northern BESS A was operating in both directions. The feeding direction for curative operation is partly reversed compared to the initial VPL operating point. The southern BESS K was almost exclusively feeding into the grid.

In general, most congestion in the German transmission grid occurs in the northern and central regions due to the high infeed of renewables. Therefore, having BESS A feed in power in a GB setup may seem counterintuitive, as this could aggravate congestion in the south. However, this may be a feasible and beneficial solution as more OW curtailment can be used, which may have a higher impact on congested lines than GBs. In real-world applications, such CM schemes may be discarded as they lead to counterintuitive power flows, increasing power flows on uncongested lines.

Curative measures can influence congested lines either directly or indirectly. The power flow can be directly controlled if a sensitivity exists between the node/PST affected by CM measures and a congested branch. In case of no existing sen-

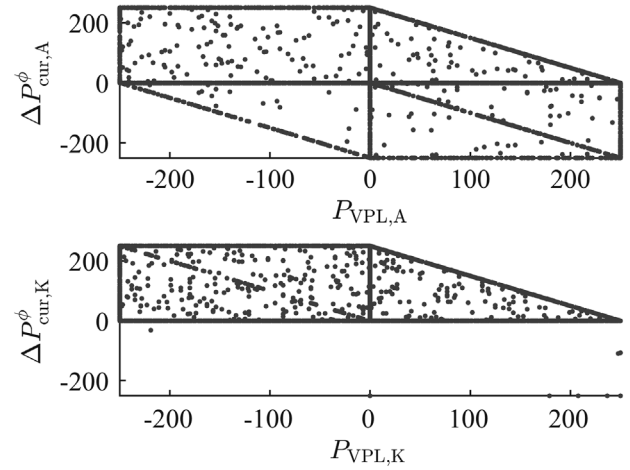


FIGURE 11 VPL versus curative GB set points for BESS in Audorf (A) and Kupferzell (K) for Scenario 3b.

sitivity on congested branches, measures can still impact remote power flows indirectly, for example, by acting as a balancing counterpart for remote units.

The impact of a curative measure of unit u was measured by calculating the power flow shifts $\Delta s_{cur,u}^\phi$ on all CBs using the OTDF and OSDF sensitivities for the corresponding contingency ϕ (see (43)).

$$\Delta s_{cur,u}^\phi = \text{otdf}_u^\phi \cdot \Delta p_{cur,u}^\phi \quad (43)$$

$$\forall b \in \mathcal{M}_B, \forall u \in \mathcal{M}_U, \forall \phi \in \mathcal{M}_U$$

For PSTs (44) applies:

$$\Delta s_{cur,p}^\phi = \text{osdf}_p^\phi \cdot \Delta \theta_{cur,p}^\phi \quad (44)$$

$$\forall b \in \mathcal{M}_B, \forall u \in \mathcal{M}_U, \forall \phi \in \mathcal{M}_U$$

To quantify the congestion relief by each unit and curative measure, the power flow shifts $\Delta s_{cur,u}^\phi$ were subtracted from the power flow $s_{cur}^{(n-1),\phi}$ in ‘ $(n-1)$ -cur.’-state. The remaining overload was the relief $r_{cur,u}^\phi$ (see (45)):

$$r_{cur,[u,p]}^\phi = \max \left\{ \begin{array}{l} \left\| s_{cur}^{(n-1),\phi} - \Delta s_{cur,[u,p]}^\phi \right\| - s_b^{\text{PATL}} \\ 0 \end{array} \right. \quad (45)$$

$$\forall b \in \mathcal{M}_B, \forall u \in \mathcal{M}_U, \forall \phi \in \mathcal{M}_U \forall p \in \mathcal{M}_P$$

Figure 12 displays the cumulated reliefs induced by the different curative CM measure types. The 10 installed PSTs accounted for the most significant curative reliefs, followed by the four HVDC links. Even if the direct relief by GB is minimal, they support using OW. In Scenario 4, the relief created OW (2.8 TW) approaches the relief of HVDC (3.6 TW). This comparably slight difference is remarkable when comparing

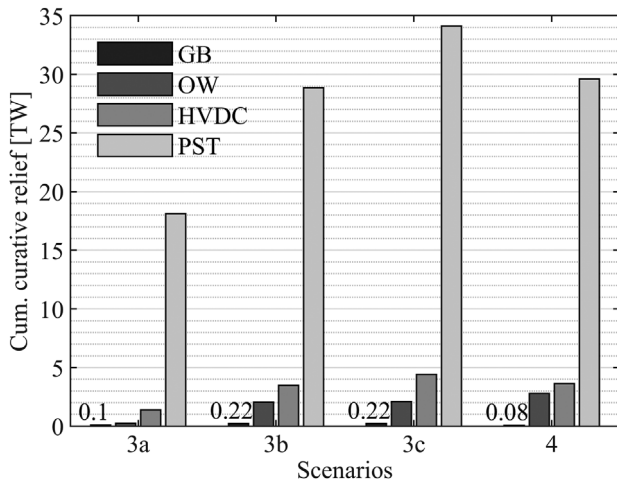


FIGURE 12 Cumulated curative relief r_{cur}^{ϕ} by CM measure type

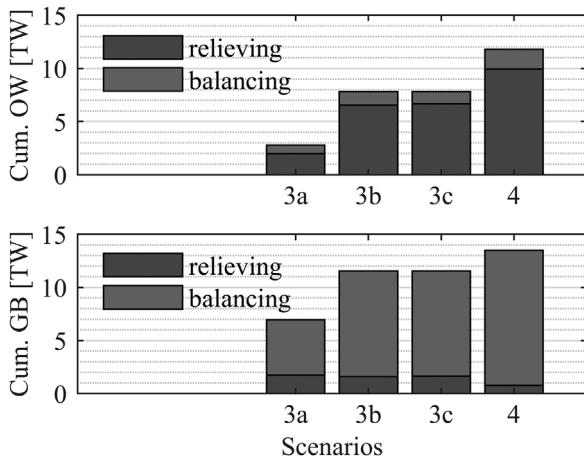


FIGURE 13 Shares of cumulated curative OW and GB power with directly relieving impact and balancing effect

the maximal possible set point ranges per contingency of OW and HVDC. For OW, 500 MW could be curtailed (supported by 2•250 MW GB power). The four HVDC inverters with a rated power of 2 GW each would have been able to shift their operating points by 16 GW in total.

The support of GBs for the relief by OW curtailment is confirmed in Figure 13. The used power from GB or OW units in each contingency was classified as ‘relieving’ if the particular set point adjustment induced a direct relief on at least one branch. If no branch was affected by the unit, the used power was classified as ‘balancing’. Figure 12 proves that OW was predominantly used for relieving in all scenarios, while GBs were most often used for balancing.

In summary, the simulation results prove the advantages of curative CM concerning the volume of costly preventive CM measures. TATL limits for a 2-min timeframe are only rarely binding and could be restricted to a subset of endangered branches. The investigated configuration of two BESSs with 250 [MW, MWh] each and locations in Audorf and Kupferzell should be used for GB purposes rather than for a VPL. Cur-

rently, the two BESSs are part of different pilot setups without interaction. The simulations, therefore, gave an outlook on a joint operation of different BESSs. Because of the high share of GB power used for balancing OW curtailment, a relocation of BESSs towards congested corridors in the south should be considered. The relocation suggestion applies especially to the BESS in Audorf.

6.4 | Computational burden and complexity

The size of the linear program for the VPL (6)–(10) increases linearly in terms of considered branches \mathcal{M}_b , time steps \mathcal{M}_t , and storages \mathcal{M}_s . LPs in general can be solved in polynomial time [40]. The optimization problem for the VPL was solved using the Gurobi solver [41] on a Windows Workstation with an AMD Ryzen 7502P 32-Core CPU and 256 GB RAM in approx. 6 h. The effect of additional branches on the computing time depends on the grid topology and solver parameters.

The complexity of the CM optimization problem depends mainly quadratically on the number of branches \mathcal{M}_b , since each branch is a potential contingency in \mathcal{M}_ϕ leading to a new grid topology, which needs to be considered in the optimization. In terms of time steps \mathcal{M}_t , units \mathcal{M}_U , and PST \mathcal{M}_P there is a linear dependency with the problem size.

In practice, contingency filtering permits retaining a reasonable problem size. The resulting LP formulation can also be solved in polynomial time.

7 | REAL-TIME APPLICATION CONCEPT

As the previous sections show, curative CM effectively reduces the need for redispatch. However, since the measures are calculated during planning processes in advance, curative CM is subject to uncertainties, which results in the question of how to respond to varying grid conditions. One possibility is the ad-hoc calculation of curative measures after the occurrence of the contingency. These measures are defined as *curative ad-hoc measures* (cAHM). Since they are calculated after a contingency occurs, the calculation needs to be robust and fast. Hence, a heuristic approach is proposed. Figure 14 depicts a heuristic algorithm that can be used to determine cAHM.

When starting the algorithm after the occurrence of a contingency, power flows need to be calculated, and all available measures and their possible set points must be known. These calculations are only executed once at the beginning of the algorithm. This information allows for calculating sensitivities and the maximum power flow shifts on the congested lines. Subsequently, the algorithm prioritizes measures. Measures with opposing effects on different congestions can be excluded during the sorting process to avoid the aggravation of other congestions. After the prioritization, the system operator or an automated system triggers the measures. One measure after

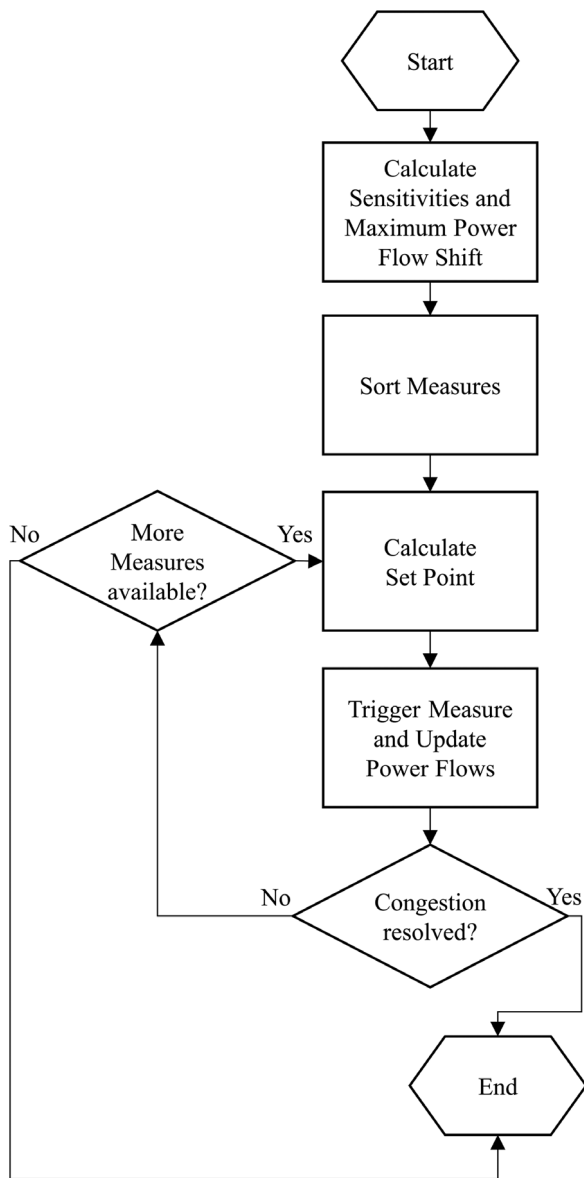


FIGURE 14 Calculation of curative ad-hoc measures

another is applied until the congestion is resolved or until no measures are left.

Besides using cAHM to respond to uncertainties of forecasts, the concept could also provide additional backup if a pre-calculated CM measure cannot be activated as planned. In either scenario, the consideration of thermal limits is vital. Since the calculations run after unforeseen contingencies, there might be only limited time left to implement cAHM before assets overheat. The tool presented in [13] provides methods to determine the remaining timeframe until an OHL reaches its maximum temperature.

The explained method was developed for a centralized control scheme. While centralized solutions are a realistic approach for integration into current control schemes, this might change in the future. More decentralized and automated solutions seem to be more likely. While CM today is mainly

performed manually—albeit supported by software tools—the limited timeframes available for activating curative and especially ad-hoc measures suggest using an automated CM system. Distributed control concepts offer a more robust solution than the status-quo centralized controls. These may become a single point of failure for time-critical applications. One implementation of such distributed control is a Multi-Agent System (MAS). Due to the absence of a single point of failure, they also scale well for application in different grids or during topology changes and offer improved efficiency by parallelizing computation efforts [42].

The authors of this paper participated in developing several MASs for operational CM over the last decade. Although BESSs have not been explicitly considered within those works, they could be integrated into the existing structures reasonably quickly. Thus a brief, qualitative evaluation thereof is presented in the following paragraph.

While the used measures differ from power flow control devices [43, 44] to PSTs [45] and generation redispatch [46, 47] and HVDC paths [48], the overall concept is similar: Each substation in the grid is equipped with a software agent that monitors grid equipment in its vicinity. Moreover, the agent can autonomously change specific device set points and exchange information with other agents, thus achieving coordination of CM measures. The heuristic algorithm proposed in Figure 13 can be included in such a MAS to form an automated distributed control system. Calculation of sensitivities and maximum power flow shifts can be distributed among all agents with access to a BESS. To ensure balanced-out BESS utilization according to constraint (6) and avoid overcompensation of existing congestions, agents can then negotiate the best course of actions among each other, similar to [44, 46, 47]. With modern ICT solutions, the agent-to-agent communication delay is expected to be outweighed by reductions in cAHM activation times due to parallelized computations. In fact, in the previous laboratory works by the authors, agents solved congestions within several seconds, using flexible generators and loads instead of BESSs [44]. Furthermore, the scalability of MASs makes the system robust towards communication outages and power grid topology changes. Hence, the authors want to include the utilization of BESSs within the existing MAS in future works.

8 | CONCLUSION AND OUTLOOK

This paper integrated grid-scale BESSs into preventive and curative CM optimization. The results demonstrated that BESSs reduce the congestion work and redispatch volume in their preventive and curative applications as VPL and their curative application as GBs. The authors chose to use BESSs, which are planned for the German transmission grid. In this scenario, using the BESSs as GBs was more effective than their application as VPL. These findings indicate an advantage of curative BESS use but might be attributable to other factors, such as the location of the BESSs. Further research regarding the optimal placement of BESSs for CM must be realized to find a definitive answer.

Another important result of this paper is the influence of external limits compared to the thermal limits of OHL. Capping the maximum permissible current at 3.6 kA significantly constrained the potential of curative measures. At the same time, thermal constraints were only rarely binding for TATL time-frames of 2 min. These results further stress the importance of external current limits in transmission grids and the need for further research on their expansion.

This paper considered two BESSs for both operation strategies. However, further research with more storage facilities is necessary to verify the results further. Also, $(n-1)$ calculations for the VPL algorithm are required for actual transmission system operation. Furthermore, including ancillary services in operation strategies for grid-scale BESSs, while securing availability for CM, has to be further researched.

Finally, this paper introduced concepts for the real-time application of curative CM. In upcoming research, these need to be included in existing CM processes to evaluate their performance and compare them to current processes.

AUTHOR CONTRIBUTIONS

Martin Lindner: Conceptualization, Data curation, Formal analysis, Investigation, Methodology, Project administration, Software, Validation, Visualization, Writing – original draft, Writing – review & editing. Jan Peper: Conceptualization, Data curation, Formal analysis, Investigation, Methodology, Software, Validation, Visualization, Writing – original draft, Writing – review & editing. Nils Offermann: Conceptualization, Data curation, Formal analysis, Investigation, Methodology, Software, Validation, Visualization, Writing – original draft, Writing – review & editing. Charlotte Biele: Conceptualization, Data curation, Methodology, Software, Visualization, Writing – original draft, Writing & review & editing. Milijana Teodosic: Conceptualization, Methodology, Visualization, Writing – original draft, Writing – review & editing. Oliver Pohl: Conceptualization, Methodology, Visualization, Writing – original draft, Writing – review & editing. Julian Menne: Data curation, Methodology, Software. Ulf Häger (GE): Supervision, Writing – original draft, Writing – review & editing.

ACKNOWLEDGEMENTS

The authors gratefully acknowledge the computing time provided on the Linux HPC cluster at Technical University Dortmund (LiDO3), partially funded in the course of the Large-Scale Equipment Initiative by the German Research Foundation (DFG) as project 271512359. We acknowledge financial support by DFG and TU Dortmund University within the funding programme Open Access Costs.

CONFLICTS OF INTEREST

Dr. Ulf Häger is the Guest Editor of IET's Special Issue on 'Recent Trends of Power Flow Control in Power System Networks'.

DATA AVAILABILITY STATEMENT

The data that support the findings of this study are available from the corresponding author, ML, upon reasonable request.

ORCID

Martin Lindner  <https://orcid.org/0000-0001-8466-2666>

Oliver Pohl  <https://orcid.org/0000-0002-3874-9362>

REFERENCES

- Guideline on capacity allocation and congestion management: 2015/22; 24 Jul 2015 [cited 2 Jun 2022]. <https://eur-lex.europa.eu/legal-content/EN/TXT/?uri=CELEX:32015R1222>.
- Guideline on electricity transmission system operation: 2017/1485; 2 Aug 2017 [cited 30 Apr 2021]. <https://eur-lex.europa.eu/legal-content/EN/TXT/?uri=celex%3A32017R1485>.
- Westermann, D., Schlegel, S., Sass, F., Schwerdfeger, R., Wasserrab, A., Haeger, U., et al.: Curative actions in the power system operation to 2030. In: International ETG-Congress 2019; ETG Symposium, pp. 1–6 (2019).
- van Acker, T., van Herfem, D.: Linear Representation of Preventive and Corrective Actions in OPF Models. IEEE IAS/PELS/PES Benelux Chapter; Eindhoven; 2016.
- Deutsches Grenzwertkonzept; November 2021 [cited 5 May 2022]. https://www.netztransparenz.de/portals/1/%c3%9cNB-DeutschesGrenzwertkonzept_202111.pdf.
- IEEE Power & Energy Society: Institute of Electrical and Electronics Engineers; IEEE-SA Standards Board. IEEE standard for calculating the current-temperature relationship of bare overhead conductors. New York: Institute of Electrical and Electronics Engineers; 2013. <http://ieeexplore.ieee.org/servlet/opac?punumber=6692856>.
- WG B2.43: GUIDE FOR THERMAL RATING CALCULATIONS OF OVERHEAD LINES: Technical Brochure 601. Paris: CIGRE; 2014 [cited 14 Oct 2020]. <https://e-cigre.org/publication/601-guide-for-thermal-rating-calculations-of-overhead-lines>.
- Fang, D., Gunda, J., Zou, M., Harrison, G., Djokic, S.Z., Vaccaro, A.: Dynamic thermal rating for efficient management of post-contingency congestions. In: Power Tech Conference. Milano: [s. n.]; pp. 1–6 (2019).
- Banakar, H., Alguacil, N., Galiana, F.D.: Electrothermal coordination part I: Theory and implementation schemes. IEEE Trans. Power Syst. 20(2), 798–805 (2005).
- Wang, M.-X., Han, X.-S.: Study on electro-thermal coupling optimal power flow model and its simplification. In: 2010 IEEE Power and Energy Society general meeting: IEEE PES-GM 2010, Minneapolis, Minnesota, USA, 25–29 July 2010. Piscataway, NJ: IEEE, pp. 1–6 (2010).
- Bucher, M.A., Andersson, G.: Robust corrective control measures in power systems with dynamic line rating. IEEE Trans. Power Syst. 31(3), 2034–2043 (2016).
- Kollenda, K., Schrief, A., Biele, C., Lindner, M., Sundorf, N., Roehder, A. et al.: Curative measures identification in congestion management exploiting temporary admissible thermal loading of overhead lines. IET Gener. Transm. Distrib. 16 (2022).
- Biele, C., Lindner, M., Mees, S., Rehtanz, C.: Simulation tool for the transient temperature behavior of overhead line conductors. In: Schulz D (ed.) NEIS 2022: Conference on Sustainable Energy Supply and Energy Storage Systems Hamburg, 26–27 September 2022. 1. Neuerscheinung, Berlin: VDE Verlag (2022).
- Gutermuth, G., Giuntoli, M.: Network operator owned storages as an option for congestion management. In: 2020 IEEE PES Innovative Smart Grid Technologies Europe (ISGT-Europe). IEEE, pp. 1074–1078 (2020).
- Keyvani, B., Flynn, D.: Coordinated investment in wind-rich regions using dynamic line rating, energy storage and distributed static series compensation to facilitate congestion management. IET Renewable Power Gen 16(9), 1882–1896 (2022).
- Huang, Y., Hu, W., Min, Y., Zhang, W., Luo, W., Wang, Z., et al.: Risk-constrained coordinative dispatching for battery energy storage systems of wind farms. In: 2013 IEEE PES Asia-Pacific Power and Energy Engineering Conference (APPEEC). IEEE, pp. 1–6 (2013).
- Islam, S.: Challenges and opportunities in grid connected commercial scale PV and wind farms. In: 2016 9th International Conference on Electrical and Computer Engineering (ICECE). IEEE, pp. 1–7 (2016).
- Moradzadeh, M., van de Vyver, J., Vandeveld, L.: Optimal energy storage sizing based on wind curtailment reduction. In: 2014 International

- Conference on Renewable Energy Research and Application (ICRERA). IEEE, pp. 331–335 (2014).
19. Vargas, L.S., Bustos-Turu, G., Larrain, F.: Wind power curtailment and energy storage in transmission congestion management considering power plants ramp rates. *IEEE Trans. Power Syst.* 30(5), 2498–2506 (2015).
 20. Yan, X., Gu, C., Zhang, X., Li, F.: Robust optimization-based energy storage operation for system congestion management. *IEEE Syst. J.* 14(2), 2694–2702 (2020).
 21. RTE: Rationalizing the way in which the grid is operated [cited 21 May 2022]. <https://www.rte-france.com/en/accelerate-energy-transition/rationalised-use-grid>.
 22. IRENA: Virtual Power Lines: Innovation Landscape Brief. Abu Dhabi (2020) [cited 22 Sep 2021]. https://www.irena.org/-/media/Files/IRENA/Agency/Publication/2020/Jul/IRENA_Virtual_power_lines_2020.pdf.
 23. Del Rosso, A.D., Eckroad, S.W.: Energy storage for relief of transmission congestion. *IEEE Trans. Smart Grid* 5(2), 1138–1146 (2014).
 24. Wen, Y., Guo, C., Kirschen, D.S., Dong, S.: Enhanced security-constrained OPF with distributed battery energy storage. *IEEE Trans. Power Syst.* 30(1), 98–108 (2015).
 25. Wen, Y., Guo, C., Pandzic, H., Kirschen, D.S.: Enhanced security-constrained unit commitment with emerging utility-scale energy storage. *IEEE Trans. Power Syst.* 31(1), 652–662 (2016).
 26. Cao, J., Du, W., Wang, H.F.: An improved corrective security constrained OPF with distributed energy storage. *IEEE Trans. Power Syst.* 31(2), 1537–1545 (2016).
 27. Cao, J., Liu, Y., Ge, Y., Cai, H., Zhou, B.W.: Enhanced corrective security constrained OPF with hybrid energy storage systems. In: 2016 UKACC 11th International Conference on Control (CONTROL). IEEE, pp. 1–7 (2016).
 28. Lindner, M., Mende, D., Wasserrab, A., Sacar, I., Ariatbar, M., Lakenbrink, C., et al.: Corrective congestion management in transmission grids using fast-responding generation, load and storage. In: 2021 IEEE Electrical Power and Energy Conference (EPEC). IEEE, pp. 1–6 (2021).
 29. Porst, J., Richter, J., Mehlmann, G., Luther, M.: Operation of grid boosters in highly loaded transmission grids. In: 2022 IEEE International Conference on Power Systems Technology (POWERCON). IEEE, pp. 1–6 (2022).
 30. *Bestätigung des Netzentwicklungsplans Strom für das Zieljahr 2035*. Bonn; Januar 2022 [cited 27 May 2022]. https://data.netzausbau.de/2035-2021/NEP2035_Bestaetigung.pdf.
 31. Wood, A.J., Wollenberg, B.F., Sheblé, G.B.: *Power Generation, Operation and Control*. 3rd ed. Hoboken: IEEE Wiley (2014). <https://search.ebscohost.com/login.aspx?direct=true&scope=site&db=nlebk&db=nlabk&AN=643518>.
 32. Spieker, C., Schwippe, J., Klein, D., Rehtanz, C. (eds.): *Transmission system congestion analysis based on a European electricity market and network simulation framework [2016 Power Systems Computation Conference (PSCC)]* (2016).
 33. Hoffrichter, A., Kollenda, K., Schneider, M., Puffer, R.: Simulation of curative congestion management in large-scale transmission grids. In: 2019 54th International Universities Power Engineering Conference (UPEC): Proceedings, 3–6 September 2019, Bucharest, Romania. Piscataway, NJ: IEEE, pp. 1–6 (2019) [cited 13 Apr 2022].
 34. Verboomen, J., van Hertem, D., Schavemaker, P.H., Kling, W.L., Belmans, R.: Analytical approach to grid operation with phase shifting transformers. *IEEE Trans. Power Syst.* 23(1), 41–46 (2008).
 35. Guo, J., Fu, Y., Li, Z., Shahidepour, M.: Direct calculation of line outage distribution factors. *IEEE Trans. Power Syst.* 24(3), 1633–1634 (2009).
 36. Grundsätze für die Ausbauplanung des deutschen Übertragungsnetzes; Jul. 2020. https://www.amprion.net/Dokumente/Netzausbau/Netzplanungsgrunds%C3%A4tze/2020.07.31_Update_%C3%9CNB-PIGrS_final.pdf.
 37. Grid Development Plan 2030 (2019): Second Draft; 8 Dec 2019 [cited 11 Jun 2022]. https://www.netzentwicklungsplan.de/sites/default/files/paragraphs-files/Standard_presentation_GDP_2030_V2019_2nd_draft.pdf.
 38. European Network of Transmission System Operators for Electricity. Ten Year Network Development Plan 2020. Brussels (2021) [cited 9 Jun 2022]. https://eepublicdownloads.blob.core.windows.net/public-cdn-container/tyndp-documents/TYNDP2020/FINAL/entsoe_TYNDP2020_Main_Report_2108.pdf.
 39. Spieker, C. Europäische Strommarkt- und Übertragungsnetzsimulation zur techno-ökonomischen Bewertung der Netzentwicklung. Shaker (2019).
 40. Karmarkar, N.: A new polynomial-time algorithm for linear programming. In: *Proceedings of the Sixteenth Annual ACM Symposium on Theory of Computing - STOC '84*. New York, New York, USA: ACM Press, pp. 302–311 (1984).
 41. Gurobi Optimizer Reference Manual: Version 9.1. <https://www.gurobi.com>.
 42. Li, H., Sun, H., Wen, J., Cheng, S., He, H.: A fully decentralized multi-agent system for intelligent restoration of power distribution network incorporating distributed generations [application notes]. *IEEE Comput. Intell. Mag.* 7(4), 66–76 (2012).
 43. Hager, U., Seack, A., Rehtanz, C., Lehnhoff, S., Zimmermann, T., Wedde, H.F.: Applicability of coordinated power flow control based on multi-agent systems. In: 2010 IREP Symposium Bulk Power System Dynamics and Control - VIII (IREP 2010): [Buzios], Rio de Janeiro, Brazil, 1–6 August 2010. Piscataway, NJ: IEEE, pp. 1–8 (2010).
 44. Pohl, O., Spina, A., Häger, U.: Demonstration of automated curative power flow control with a multi-agent system using distributed series reactors in a PHIL simulation. In: *Power Systems Computation Conference (PSCC)* (2022).
 45. Dalhues, S., Robitzky, L., Häger, U., Dorsch, N., Kurtz, F., Wietfeld, C.: Analysis of real-time coordination of distributed power flow controllers using software-defined networking communication. In: 2018 IEEE Power Energy Society Innovative Smart Grid Technologies Conference (ISGT), pp. 1–5 (2018).
 46. Robitzky, L., Müller, S.C., Dalhues, S., Rehtanz, C.: Agent-based redispatch for real-time overload relief in electrical transmission systems: Denver, Colorado, USA, 26–30 July 2015. In: *IEEE Power & Energy Society General Meeting*. Denver, Colorado (2015).
 47. Pohl, O., Kentchim, R., Hito, L., Ibrahim, H., Al Samman, O., Häger, U., et al.: Integrating an autonomous agent-based power flow control system into control center software. In: *VDE ETG (ed.) VDE ETG-Congress 2021*. IEEE (2021).
 48. Müller, S.C., Häger, U., Rehtanz, C.: A multiagent system for adaptive power flow control in electrical transmission systems. *IEEE Trans. Ind. Inf.* 10(4), 2290–2299 (2014). <https://ieeexplore.ieee.org/ielx7/8889870/8893436/08893627.pdf?tp=&arnumber=8893627&isnumber=8893436&ref=aHR0cHM6Ly9pZWVleHBsb3JlLmlZlWUub3JnL2RvY3VtZW50LzgzOTM2Mjc=>.
 49. Stott, B., Jardim, J., Alsac, O.: DC Power Flow Revisited. *IEEE Trans. Power Syst.* 24(3), 1290–1300 (2009). <https://doi.org/10.1109/tpwrs.2009.2021235>

How to cite this article: Lindner, M., Peper, J., Offermann, N., Biele, C., Teodosic, M., Pohl, O., Menne, J., Häger, U.: Operation strategies of battery energy storage systems for preventive and curative congestion management in transmission grids. *IET Gener. Transm. Distrib.* 17, 589–603 (2023). <https://doi.org/10.1049/gtd2.12739>